UK Ministry of Defence © Crown Owned Copyright 2022/AWE

A route to enhanced performance for the petawatt beamlines of the Orion laser facility

E. J. Harvey

AWE, Aldermaston, Reading, RG7 4PR, UK

Abstract The Orion laser facility at AWE provides multiple beams to target delivering synchronised pulses at both nanosecond and sub-picosecond duration. In the latter peak power approaches the petawatt level. This paper presents a conceptual design for potential development of these beamlines. This would deliver a significant enhancement of performance at the fundamental. In addition, a new approach is described to the management of frequency conversion at high intensity which may allow significantly enhanced performance at the second harmonic also.

Key words: **Chirped pulse amplification, frequency doubling, temporal contrast.**

I. INTRODUCTION

Orion [1], a high power Nd:glass laser facility, commenced user experiments in 2013 [2]. It provides ten beamlines with 0.1–10ns pulse duration ("long pulse") each with a specification of 500J in 1ns at 351nm and two beamlines each with a specification of 500J in 500fs ("short pulse")

Correspondence to: E. J. Harvey, AWE, Aldermaston, Reading, RG7 4PR, UK. Email: ewan.harvey@awe.co.uk

at 1054nm. To obtain increased temporal contrast, one of the latter beamlines may be frequency doubled. With the original capability [3] enhanced recently, up to 210J in 500fs is available at 527nm [4]. For a programme of experiments at high energy density, laser pulses are delivered to a small target, positioned and synchronised to high accuracy.

The study presented here considers significant enhancement of the performance of the "short pulse" beamlines. Nominal specifications for operation at the fundamental (1ω) have been proposed by the user community, requiring an increase in pulse energy on target to 1kJ in each beamline in a duration reduced to 200–300fs. The specification at the second harmonic (2ω) is to obtain as great a proportion of this pulse energy as reasonably practicable in a duration no greater than 1ps.

A conceptual design has been developed which meets specification with the minimum of modification to the existing beamlines. To deliver the second harmonic, a relatively straightforward approach is described. However, a novel, more developed approach with the potential to deliver similar energy in a much shorter pulse has also been devised. This route to high peak power at the second harmonic is not limited to the Orion facility and could be applicable generally.

Designs have been developed with the support of numerical simulation [5]. Details of design and, for each mode of operation, an assessment of expected performance and critical specifications derived from it are presented.

II. Conceptual design—operation at 1ω

Front end

At present, the front end consists of an oscillator, pulse stretchers and pre-amplifiers based on optical parametric amplification [1]. Spectral power in the output with a 20th order supergaussian profile of 15nm FWHM has been assumed for the purposes of beamline design. It will be necessary to introduce an acousto-optic programmable dispersive filter (AOPDF) to achieve the shorter pulse duration required, through fine control of the spectral phase profile. No other modification of the front end is envisaged, except to amend the centre wavelength λ_0 of all sub-systems to 1057nm (see below), from the current value of 1054nm [1].

Rod amplifier stage

Each beamline contains two rod amplifiers which are passed twice. The two rods in each beamline differ, with one a phosphate glass (LHG-8) and the other a silicate glass (ED-2), to facilitate suitably broad bandwidth in the laser gain. While different options have been considered for reconfiguring the amplification in Nd:glass generally, requirements should be met without modifying the rod amplifier stage. The gain bandwidth may be increased sufficiently by increasing the contribution from the silicate rod amplifier. To be effective, however, this must be accompanied by a small change in the centre wavelength of sub-systems external to the laser amplifier, from 1054nm to 1057nm, so as to relax the impact of the upper bound on wavelength which arises [1].

Disc amplifier stage

The aspiration to a pulse energy on target of 1kJ in each beamline informed the original design of the facility. A vacancy was included in order to accommodate an additional amplifier at 180mm beam diameter. (Each amplifier contains three discs of LG-770.) Use of alternative glasses, such

as variants of BLG-80 [6], has been considered in the disc amplifiers, but no better compromise between output energy and bandwidth has been found.

Anticipating a change in the orientation of linear polarisation, as dictated by the pulse compression (see below), the re-mounting of relevant components is expected, after rotation about the beam axis through a right angle.

Chromatic aberration in refractive singlet lenses, used routinely in beam transport, has a significant impact on beamline performance [7–9]. This will prevent achievement of the required pulse duration and it will be necessary to correct the aberration. ~~Introduction of diffractive lenses, which show compensating aberration, is the favoured option.~~ The utility of diffractive components which show axial chromatic aberration of the opposite sign has been recognised [10–12]. Such components are established as correctors of chromatic aberration in high power beamlines such as PETAL [13] and OMEGA EP [14], and they are the favoured option for Orion. ~~This might be done~~ They might be introduced, as elsewhere, immediately prior to ~~expansion and~~ spatial filtering of the beam, at 180mm diameter or possibly earlier, at 140mm diameter, to provide for removal of small-scale phase error which may arise. While proprietary routes for manufacture are available, a collaborative programme of development is currently in progress which seeks to exploit in-house capability, enabling manufacture on site [15].

Pulse compression

At present, the pulse compression in each beamline consists of a single pair of reflection gratings. Owing to the limited threshold for laser-induced damage, it has long been understood that the gold coating represents the fundamental constraint on an increase in pulse energy. Multi-layer dielectric (MLD) gratings, which show a substantially increased damage threshold in the relevant range of

pulse duration [16], are now available at large aperture. However, it is considered likely that otherwise like-for-like replacement is not available, with the groove profile implied at the current density (1480mm^{-1} [1]) not considered viable. In any event, increased bandwidth in the amplified pulse would enlarge the aperture required at the second grating and beyond, where the beam is laterally dispersed, to an extent which would not be cost-effective.

Therefore, the grating configuration must change. Given the high cost of replacement, the existing vacuum vessels shall be retained, fixing the geometry of the beams within. To resolve this situation, accommodating gratings of different groove density and a greater bandwidth, the pulse compression in each beamline is divided between two grating pairs in sequence (see Figure 1). The second (C2 = DG3, DG4) will be accommodated within one of the existing vacuum vessels, while the first (C1 = DG1, DG2) will precede it, located in space available in the Laser Hall and not evacuated. Support structures for the latter will be sufficiently robust to enable and retain alignment of the beamlines to the tolerances required. Separation into two differing grating pairs allows the new configuration to replicate the existing spectral phase change (to second and third derivatives, at least).

Figure 1

The grating pair accommodated in the vacuum vessels (C2) must take a groove density smaller than the current value. The angle of incidence at DG3 must be comparable to the current value. If it is too small, the requirement for pulse energy cannot be met. If it is too large, the aperture of the gratings, already the largest components in the facility, becomes excessive. Together, these conditions restrict the range of practicable groove density to around 1150mm^{-1}–

1350mm^{-1}. They also imply that the angle of diffraction at DG3 is smaller than the angle of incidence, opposite to the current configuration of the pulse compression.

The additional grating pair in each beamline (C1) will be accommodated prior to the other as described above. Applying similar considerations, a higher groove density is implied and an angle of diffraction at DG1 which is larger than the angle of incidence.

The proposal is summarised in Table 1. Practicability is contingent on availability of efficient MLD gratings at these groove densities, but realistic designs have been established (see Acknowledgement). In contrast to gold coating, they require *s* polarisation. The laser-induced damage threshold required for each grating and the tolerances for misalignment have been determined (see Appendix).

Table 1

Although the complexity of the pulse compression is increased, a valuable benefit of multiple grating pairs is the option to oppose the lateral dispersions in order to reduce the effect overall. While the lateral dispersion in the compressed pulse is large at present (around 39mm nm^{-1}), in the proposed configuration it is all but eliminated, optimising spatial filling at the critical final grating and beyond. Note that, in order to do this, the two pairs must be arranged so that the beam in each tracks laterally in the same direction (see Figure 1). This arrangement also reduces the sensitivity overall to input pointing/wavefront error, for a given pulse duration.

III. Conceptual design—operation at 2ω

Frequency doubling the compressed pulse in one of the beamlines is an important aspect of facility capability. This is achieved in an auxiliary chamber separate from the compressor chambers (see

Figure 2). However, an awkward feature of both the original installation [1, 3] and the present installation, enhanced in aperture by segmentation with two beamlets 300mm square in a vertical array [4], is the fact that the frequency doubling crystals are on the verge of being over-driven [9]. Increased input intensity would lead to de-conversion and loss of efficiency. This would arise if chromatic aberration in the beamline were corrected [9], a realistic possibility in the near term in its own right [15], but much more so with the increased pulse energy and reduced pulse duration specified here for 1ω operation. In the latter case the likely consequence would be several cycles of conversion and de-conversion through the thickness of the crystals, and an unmanageable impact on laser performance.

Figure 2

Clearly, a thinner crystal would address this situation. Simulation suggests that converted pulse energy would be optimised at a reduced thickness of order 1mm. While doubling of similar [17] or much higher intensities [18, 19] in thin crystals has been investigated, no such component is available, or likely to become available in the near term, at the required aperture. Instead, consider moderating the input intensity sufficiently to regain efficient conversion in available crystals.

This could be achieved simply by reducing the pulse energy, but this is clearly a poor strategy. As the input pulse would be shorter than at present by default, the converted pulse energy would inevitably fall below the current value.

Alternatively, consider moderating the intensity at the crystals by controlling the temporal profile of the pulse (without significant loss). One obvious approach is to detune the otherwise well-compressed input pulse by mismatching the pulse stretchers and compressors. Unfortunately,

while the pulse would then be longer and less intense, it would also be chirped, with a variation of instantaneous frequency through the pulse. Phase matching, which is achieved exactly at only one frequency (or a limited number of discrete frequencies), would therefore be compromised.

Fortunately, type I doubling near 1057nm in potassium dihydrogen phosphate (KDP) shows group velocities for the coupled waves which nearly match at the phase-matching angle. Not only does this proof against loss of temporal overlap during conversion, it also renders the phase-matching angle much less sensitive to frequency. This implies resistance to chirp, with the pulse phase-matched relatively well over the whole bandwidth.

Basic scheme

For a given energy at the fundamental, there will be a corresponding detuning required to moderate the intensity at the crystals sufficiently to restore efficient conversion. The range of pulse duration permitted by the specification (up to 1ps at 2ω) allows a generous upper bound on the energy that can be utilised (see below). Just as importantly, it appears that the necessary detuning can be introduced without the accompanying chirp compromising the conversion process. In fact, still greater chirp appears to be acceptable.

This approach has the advantage of leaving the beamlines post-compressor unchanged. On the other hand, it is unlikely to offer a meaningful increase in peak power, able to deliver increased energy only in a longer pulse. (It is compatible with enlargement of the aperture, segmented with a 2x2 array of beamlets, for example, though the further uplift in pulse energy would be accompanied by some degradation of temporal contrast on target. The elimination of lateral dispersion in the compressed pulse precludes the softening of spectral clipping in the compressor otherwise derived from the roll-off to the periphery of the uncompressed spatial profile [1]. The

consequent degradation of temporal contrast is strongest in the parts of the aperture which are peripheral in the dispersion direction.)

Advanced scheme

There is a further option for the moderation of intensity at the frequency doubling crystals in which a detuned pulse, having been frequency doubled, might then be compressed fully. This contrasts with a scheme in which a well-compressed pulse is doubled in a thin crystal, and its temporal profile re-optimised subsequently after spectral amplitude and phase distortion in the crystal [17–19].

A further grating pair (C3 = DG5, DG6) is anticipated (see Figure 3). This is expected to be segmented as for the other optics in the auxiliary chamber. Other reflective components, such as multi-layer chirped mirrors or Gires-Tournois interferometers [20], are unlikely to supply sufficient chirp. Assuming a familiar z-fold involving the first diffracted order accommodated in a (replaced) auxiliary vacuum chamber, the grating separation is limited to around 720mm and the angle made between the incoming and outgoing beam at each grating may be in excess of 30°. The latter is far from ideal in typical circumstances, but efficient gratings will be assumed for the present. With the layout fixed, the groove density and angle of incidence are in a fixed relationship, effectively a single free parameter. In view of the limited flexibility, some assistance will be needed from the enhanced front end in the form of further fine adjustment of the spectral phase.

Figure 3

While only a relatively small chirp is needed to moderate the intensity sufficiently for the existing crystals, this leaves a problem for the post-conversion compressor. With the geometry

constrained, the modest compression required implies a low groove density of 500–600mm^{-1}. At the reduced wavelength of the second harmonic, such gratings admit multiple diffracted orders and an efficient grating design is unlikely. To avoid this situation, the groove density, and with it the chirp at the crystals, must be increased significantly. Based on a fixed angle between beams at the gratings of $|\psi - \theta_0| = 33.7°$, producing a lateral separation of 400mm over an axial separation of 600mm, a groove density is selected (see Table 2) which just exceeds the minimum value. Beyond that, as it is a free choice, the alternative with the lower chirp ($\psi > \theta_0$) is selected. Since the net effect requires a longer pulse at the crystals, with the input intensity moderated further, the crystal thickness must be increased to around 7mm, though this reduces the difficulty of manufacture. The increase in groove density also increases the angle of incidence to a suitable value. While the real damage threshold of potential gratings remains to be seen, avoiding a low angle of incidence is clearly preferable for energy handling.

Table 2

Frequency doubling is desirable as it enhances the temporal contrast of the compressed pulse significantly [1–3]. Introducing diffraction gratings post-conversion has the potential to degrade the contrast through scattering. The extent of this effect is not easy to predict. On the other hand, it should be noted that the zero order at DG5 will be rejected spatially, passing out of the beamline. This enhances the removal of unconverted light, handled currently with dichroic mirrors alone [4].

With the intended configuration established, an immediate concern is the availability of a design for efficient gratings. As it will be highly desirable to retain all gratings in a vertical plane, use of *s* polarisation at 1ω gratings and type I doubling implies *p* polarisation at 2ω gratings.

Fortunately, investigation suggests that a favourable, if somewhat demanding, design exists for p polarisation (see Acknowledgement). The laser-induced damage threshold required for each grating and the tolerances for misalignment have been determined (see Appendix).

For fine alignment of a parallel grating pair, angular dispersion in the transmitted beam can be used as a diagnostic of misalignment. This can be observed using a broadband beam brought to focus. At present, the front end produces broadband pulses at a repetition rate of 2Hz which are sufficiently energetic after frequency doubling in the auxiliary chamber to be detectable at focus at the target position [4]. This can continue in the advanced configuration if the pulse compression at the fundamental is re-optimised temporarily, as for operation in 1ω mode. While the converted pulse will be chirped subsequently by C3, this is inconsequential for time-integrated observation.

Though design is beyond the scope of this paper, diagnostics of the performance in 2ω mode will be provided.

Finally, it is necessary to consider the adjustment to the front end required in switching to 2ω mode. Various options are available. (i) The simplest requires an increase in the single-pass equivalent grating separation in the pulse stretcher $\Delta l_s = 70\text{mm}$, which addresses the quadratic term in the spectral phase, and optimisation of the residual cubic term using the AOPDF. (ii) Alternatively, the same effect may be achieved with a small increase of around 0.08° in the angle of incidence at the stretcher grating and a rather larger $\Delta l_s = 130\text{mm}$. The change in alignment may be facilitated straightforwardly by the introduction of a weak wedge. (iii) The detuning of the stretcher required for 2ω mode may be accommodated permanently and subtracted for 1ω mode by means of an insertable grating pair. This would be transmissive, on account of the limited grating separation.

IV. Expected performance

Performance of the beamlines at full power has been simulated. ~~Small-scale spatial modulation has~~ Wavefront error from optical components and the effect of spatial filtering have been neglected for simplicity. Background effects, such as amplified spontaneous emission (ASE), are not included. The spectral variation of diffraction efficiency has been represented in all cases. Pulse durations are rendered hereafter as effective values—that is, the integrated value of a temporal profile divided by its peak value—rather than the full width at half-maximum.

The bandwidth of spectral power expected immediately before and after the 1ω compressor is 7.9nm and 7.7nm respectively (FWHM) and 8.2nm and 8.0nm respectively (effective value).

Expected performance on target is summarised in Figure 4. For comparison, this includes the beamlines in their current configuration, and the correction of chromatic aberration (CA) as an intermediate step. While each beamline will continue to benefit from a deformable mirror in the disc amplifier stage [1], diffraction-limited performance on target cannot be assured.

Figure 4

In 1ω mode, some 1070J in 290fs (3.7PW and up to $2.7 \times 10^{22}\mathrm{Wcm}^{-2}$ peak) is expected on target. This meets the specification, and represents a substantial uplift in peak power and intensity.

In 2ω mode, performance depends on which option has been selected. (i) In the basic scheme, the change in effective stretcher grating separation Δl_s is set, for a given energy at the fundamental, to maximise pulse energy on target. Although a choice is available, $\Delta l_s < 0$ is favoured as it leads to a slightly steeper rising edge on the compressed pulse. The beamline is able to operate with up to 90% of full energy in the compressed pulse before the adjustment required (Δ

$l_s = -5.5\text{mm}$) reaches the upper bound on pulse duration of 1ps. At this point, up to 550J (550TW peak power) is expected on target. Within that limit, a range of performance is available, with less energy in shorter pulses (see Figure 4), which may suit some experimental requirements. However, with existing performance expected to be around 270J in 550fs (490TW peak power), the peak power is increased only marginally. (ii) In the advanced scheme, up to 550J in 150fs (3.6PW and up to $6.4 \times 10^{22}\text{Wcm}^{-2}$ peak) is expected on target. The pulse duration is reduced significantly after doubling of the frequency bandwidth and fine optimisation of the spectral phase, consistent with other studies [17–19]. Relative to the peak, the expected contrast in power is at least 8.0, 9.5 and 11.0 orders of magnitude at -5ps, -10ps and -20ps respectively. The performance that may be available in terms of pulse energy, and power and intensity with high temporal contrast, is remarkable.

V. Conclusions

Enhancement of the Orion laser facility has been considered and a conceptual design for modification of the "short pulse" beamlines has been described. This meets a proposed specification, with operability expected to remain within reasonable bounds.

The expected performance represents a substantial uplift in capability, especially if the advanced scheme for the second harmonic is implemented. While practicability of critical components is not yet confirmed, this scheme is potentially applicable quite generally. It offers a route to ultra-high power at the second harmonic, with the accompanying advantage of high temporal contrast.

Appendix I. Derived specifications

While the beamline design has been developed taking account of critical parameters, some formal requirements arise naturally from the expected performance.

Laser-induced damage threshold

Expectations of compressor gratings (see Table 3) are reasonable in C1 and C2 [16]~~, though they may be challenging in C3 in view of the reduced wavelength~~. Prospects for C3 are not known with certainty. While there is good experience of MLD gratings operating at 1ω with ps and sub-ps pulses, no examples operating in the visible spectrum are known. Adverse scaling of damage threshold with wavelength and pulse duration is foreseeable. On the other hand, *p* polarisation is specified for C3 (see Table 2). A significantly greater damage threshold for a MLD grating has been observed with *p* polarisation compared with the more usual *s* polarisation [21]. Manufacture and testing of sample gratings suitable for C3 offers a clear route to reduction of uncertainty.

It is believed that available damage thresholds will be sufficient elsewhere in the beamline.

Table 3

Tolerances for misalignment

Misalignment of the beamline in various ways leads to a potentially significant reduction in output performance. The effects have been surveyed in relevant parameter spaces by adding the appropriate spectral phase errors.

Output near the transform limit

This applies to operation in 1ω mode and in 2ω mode in the advanced scheme. For full power shots, estimates for selected tolerances are shown in Tables 4–7.

Tolerances for parallelism (grating pointing) in pulse compressors are shown in Table 4. With the spectral phase errors arising from misalignment varying linearly with position in the aperture, simple analysis implies that the tolerances should vary essentially in proportion to pulse duration. The requirements are clearly more challenging than at present, but should be manageable. They are relaxed in C3, as expected from the small size of this compressor.

Table 4

Tolerances for grating separation are shown in Table 5. With the spectral phase arising from mis-setting being spatially uniform, simple analysis implies that the tolerance should vary quadratically with pulse duration. All should be manageable physically, though in 2ω mode those for the stretcher and C1 are rather tight, the former compounded by the multi-pass configuration [1].

Table 5

Tolerances for beam pointing into the 1ω pulse compression are shown in Table 6. Once again, spectral phase error is spatially uniform and tolerances are expected to vary quadratically with pulse duration. However, the consequent reduction in the proposed configuration is offset by the deliberate opposition of the two grating pairs, in which the angles of incidence vary with pointing error in the plane of dispersion in opposite senses. In 2ω mode, tolerances on the pointing into C3 only (not shown) are particularly relaxed (>20mrad).

Table 6

Tolerances for the angle between the beam within the frequency doubling crystals and the optical axis of the material are shown in Table 7. Unfortunately, as the latter also lies in a horizontal plane, the pointing error to which the grating pairs are more sensitive is also that to which the crystals are more sensitive.

Table 7

Output away from the transform limit

This applies to operation in 2ω mode in the basic scheme. Though it is a simple approach to mitigation of excessive intensity at the existing frequency doubling crystals, it is complicated by operation away from the transform limit. For a given drive, there is a significant difference in the settings of pulse compression which maximise energy (the default) and peak power on target (and in the tolerances which arise at each setting). A compromise setting may be appropriate. Some judgment may be exercised on the optimum setting for a given experiment.

Tolerances in peak power are generally comparable with the advanced scheme (except for grating pointing out of plane, which is several times more relaxed). However, a compromise setting reduces the tolerance of both energy and peak power to pointing of the frequency doubling crystals by approximately half.

Acknowledgement

Work relating to the design and expected performance of gratings in the proposed configuration was undertaken by Plymouth Grating Laboratory. This is gratefully acknowledged.

References

[1] N. W. Hopps, K. Oades, J. Andrew, C. Brown, G. Cooper, C. Danson, S. Daykin, S. Duffield, R. Edwards, D. Egan, S. Elsmere, S. Gales, M. Girling, E. Gumbrell, E. Harvey, D. Hillier, D. Hoarty, C. Horsfield, S. James, A. Leatherland, S. Masoero, A. Meadowcroft, M. Norman, S. Parker, S. Rothman, M. Rubery, P. Treadwell, D. Winter, and T. Bett, Plasma Phys. Control. Fusion **57**, 064002 (2015).

[2] D. J. Hoarty, P. Allan, S. F. James, C. R. D. Brown, L. M. R. Hobbs, M. P. Hill, J. W. O. Harris, J. Morton, M. G. Brookes, R. Shepherd, J. Dunn, H. Chen, E. Von Marley, P. Beiersdorfer, H. K. Chung, R. W. Lee, G. Brown, and J. Emig, High Energy Density Physics **9**, 661 (2013).

[3] D. Hillier, C. Danson, S. Duffield, D. Egan, S. Elsmere, M. Girling, E. Harvey, N. Hopps, M. Norman, S. Parker, P. Treadwell, D. Winter, and T. Bett, Appl. Opt. **52**, 4258 (2013).

[4] S. Parker, C. Danson, D. Egan, S. Elsmere, M. Girling, E. Harvey, D. Hillier, D. Hussey, S. Masoero, J. McLoughlin, R. Penman, P. Treadwell, D. Winter, and N. Hopps, High Power Laser Sci. Eng. **6**, e47 (2018).

[5] E. J. Harvey, "Simulation of laser beamlines based on chirped pulse amplification", in proceedings of International Conference on Ultra-High Intensity Lasers 2006.

[6] Schott AG, "BLG-80 Broadband Laser Glass", from www.schott.com/en-gb/products/laser-materials-and-components/downloads (January 2018).

[7] Z. Bor, J. Mod. Opt. **35**, 1907 (1988).

[8] E. J. Harvey, "Performance of the main short pulse beamlines of Orion at 1ω", in AWE Plasma Physics Department Annual Report 2006, p. 35. [Copies of the report may be obtained from the Corporate Communications Office at the Atomic Weapons Establishment, Aldermaston, Reading, Berkshire, RG7 4PR, UK.]

[9] E. J. Harvey, "Physics design of the frequency doubling crystals for the main short pulse beamlines of Orion", in AWE Plasma Physics Department Annual Report 2007, p. 27. [Copies of the report may be obtained from the Corporate Communications Office at the Atomic Weapons Establishment, Aldermaston, Reading, Berkshire, RG7 4PR, UK.]

[10] Z. Bor, Opt. Lett. **14**, 119 (1989).

[11] H.-M. Heuck, P. Neumayer, T. Kühl, and U. Wittrock, Appl. Phys. B **84**, 421 (2006).

[12] J. Néauport, N. Blanchot, C. Rouyer, and C. Sauteret, Appl. Opt. **46**, 1568 (2007).

[13] N. Blanchot, G. Behar, T. Berthier, E. Bignon, F. Boubault, C. Chappuis, H. Coïc, C. Damiens-Dupont, J. Ebrardt, Y. Gautheron, P. Gibert, O. Hartmann, E. Hugonnot, F. Laborde, D. Lebeaux, J. Luce, S. Montant, S. Noailles, J. Néauport, D. Raffestin, B. Remy, A. Roques, F. Sautarel, M. Sautet, C. Sauteret, and C. Rouyer, Plasma Phys. Control. Fusion **50**, 124045 (2008).

[14] D. N. Maywar, J. H. Kelly, L. J. Waxer, S. Morse, I. A. Begishev, J. Bromage, C. Dorrer, J. L. Edwards, L. Folnsbee, M. J. Guardalben, S. D. Jacobs, R. Jungquist, T. J. Kessler, R. W. Kidder, B. E. Kruschwitz, S. J. Loucks, J. R. Marciante, R. L. Mccrory, D. D. Meyerhofer, A. Okishev, J. B. Oliver, G. Pien, J. Qiao, J. Puth, A. Rigatti, A. W. Schmid, M. J. Shoup, C. Stoeckl, K. A. Thorp, and J. Zuegel, J. Phys.: Conf. Ser. **112**, 032007 (2008).

[15] E. J. Harvey, D. A. Egan, R. J. S. Aulsberry, and S. J. Wheeler, "In-house manufacture of diffractive Fresnel lenses for correction of chromatic aberration", Poster presentation to International Conference on Ultra-High Intensity Lasers 2018.

[16] J. Neauport, E. Lavastre, G. Razé, G. Dupuy, N. Bonod, M. Balas, G. de Villele, J. Flamand, S. Kaladgew, and F. Desserouer, Opt. Expr. **15**, 12508 (2007).

[17] S. Yu. Mironov, J. Wheeler, R. Gonin, G. Cojocaru, R. Ungureanu, R. Banici, M. Serbanescu, R. Dabu, G. Mourou, and E. A. Khazanov, Quantum Electron. **47**, 173 (2017).

[18] S. Mironov, V. Lozhkarev, V. Ginzburg, I. Yakovlev, G. Luchinin, E. Khazanov, A. Sergeev, and G. Mourou, Proc. SPIE **7721**, 77211R (2010).

[19] S. Yu. Mironov, V. V. Lozhkarev, V. N. Ginzburg, I. V. Yakovlev, G. Luchinin, A. Shaykin, E. A. Khazanov, A. Babin, E. Novikov, S. Fadeev, A. M. Sergeev, and G. A. Mourou, IEEE J. Sel. Topics Quant. Electron. **18**, 7 (2012).

[20] J. Kuhl and J. Heppner, IEEE Trans. Quant. Electron. **22**, 182 (1986).

[21] S. Hocquet, J. Neauport, and N. Bonod, Appl. Phys. Lett. **99**, 061101 (2011).

Figures and tables

Figure 1

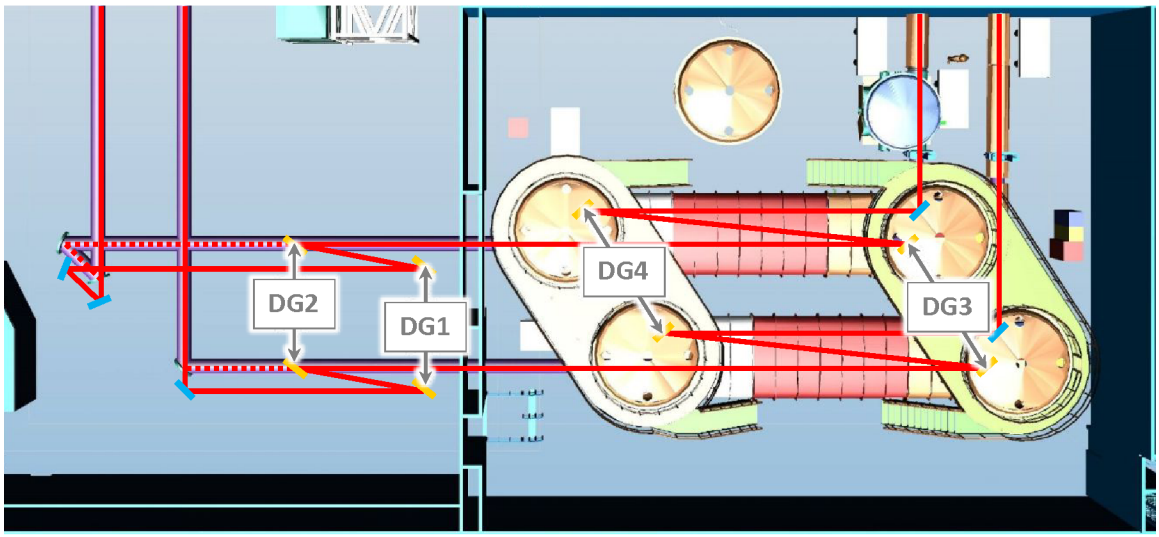

Figure 2

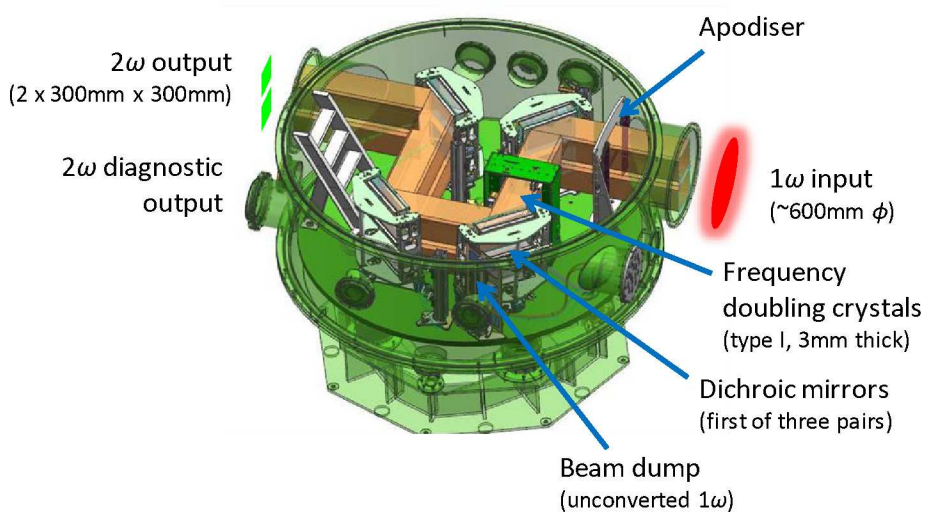

Figure 3

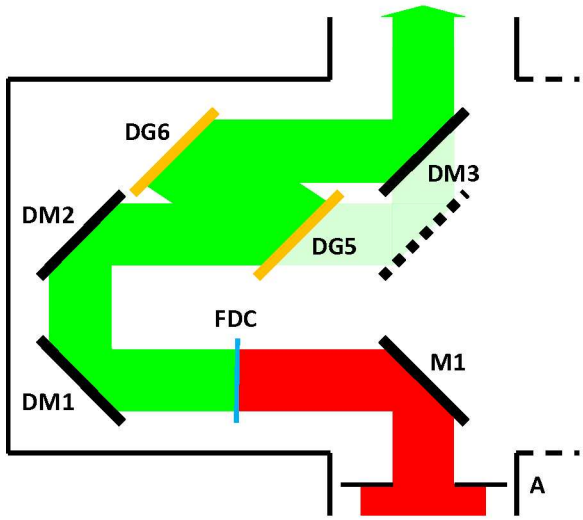

Figure 4

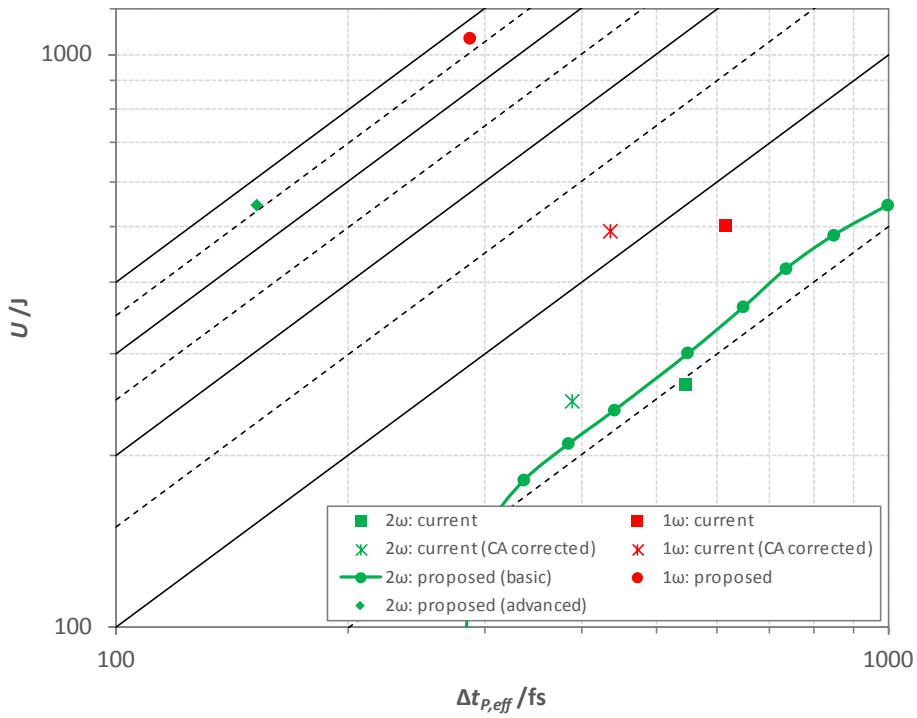

Table 1

		λ_0 /nm	Type	σ /mm^{-1}	ψ /°	θ_0 /°	w /mm	l /m
Existing configuration		1054	Gold, *p*	1480	47.9	54.9	940	13
Proposed configuration	**C1**	1057	MLD, *s*	1568	52.2	60.1	1020	5.1
	C2			1300	47.0	40.0	910	13

Table 2

λ_0 /nm	Type	σ /mm^{-1}	ψ /°	θ_0 /°	w /mm	l /m
528.5	MLD, *p*	1610	43.2	9.5	440	0.721

Table 3

Component	Fluence /mJcm^{-2}	Pulse duration	Spectral range /nm
DG1	510	2.4ns	1047–1067
DG2	490	1.0ns	
DG3	510		
DG4	490	290fs–13ps	
DG5	450	13ps	524–534
DG6	440	150fs	

Table 4

		In plane of dispersion		Out of plane of dispersion	
		1ω mode	**2ω mode**	**1ω mode**	**2ω mode**
Current	DG1	28	24	130	100
	DG2	91	80		
Proposed	DG1	14	9.2	40	19
	DG2	28	21		
	DG3	36	23	99	47
	DG4	63	45		
	DG5	N/A	760	N/A	1300
	DG6	N/A	760		

Table 5

		1ω mode	2ω mode
Current	Stretcher	2.7	2.6
	Compressor		
Proposed	Stretcher	1.2	0.66
	C1	0.80	0.45
	C2	2.7	1.5
	C3	N/A	6.8

Table 6

	In plane of dispersion /µrad		Out of plane of dispersion /mrad	
	1ω mode	2ω mode	1ω mode	2ω mode
Current	42	42	5.8	5.6
Proposed	33	19	3.7	2.8

Table 7

	Energy	Peak power
Current	140	110
Proposed	150	160

Figure and table captions

Figure 1 caption

Schematic layout (plan view) of the Laser Hall (left) and Compressor Hall (right) showing the new beam paths and components overlaid on the existing equipment. (Where they differ, the existing beam paths are shown with dashed lines.)

Figure 2 caption

Auxiliary vacuum chamber in its present configuration.

Figure 3 caption

Schematic layout (plan view) of the amended auxiliary chamber configured for 2ω mode, for one beamline only, showing the incoming beam at 1ω (red) and the continuing beam at 2ω (green). The post-conversion grating pair (DG5, DG6) has been added and the final dichroic mirror in the chamber (DM3) has been repositioned as shown (compare Figure 2). To revert to 1ω mode, the unnecessary apodiser (A) and mirrors (M1 and DM3) are removed, allowing the full aperture beam to propagate straight through the vessel.

Figure 4 caption

Expected performance on target of current and proposed configurations, showing pulse energy U and effective pulse duration of power $\Delta t_{P,eff}$ on logarithmic scales. In 2ω mode, the basic scheme is illustrated with a representative set of configurations. Loci of fixed peak power (in whole and half PW increments) are shown for reference.

Table 1 title

Draft specifications for 1ω diffraction gratings

Table 1 caption

Specifications show groove density σ, angles of incidence and diffraction at the first grating ψ and θ_0 respectively, clear width w (based on 620mm in the plane of the undispersed beam) and grating separation l. For the purposes of simulation, a circular clear aperture, truncated horizontally to top and bottom to a height of 620mm, is used for the existing configuration; a rectangular aperture of the same height is assumed for the proposed configuration.

Table 2 title

Draft specifications for 2ω diffraction gratings

Table 2 caption

Specifications show groove density σ, angles of incidence and diffraction at the first grating ψ and θ_0 respectively, clear width w (based on 320mm in the plane of the undispersed beam) and grating separation l. The clear aperture should be rectangular.

Table 3 title

Thresholds for laser-induced damage required of diffraction gratings

Table 3 caption

Thresholds are based on 50% contingency above the peak fluence in the beam, excluding small-scale spatial modulation, measured in the plane of the component.

Table 4 title

Estimated tolerances (/μrad) for grating pointing (parallelism) in 1ω mode and 2ω mode in the advanced scheme

Table 4 caption

Tolerances are based on a nominal 10% loss of peak power on target. With gratings mounted with grooves vertical, the tolerances in and out of the plane of dispersion relate to the angles of azimuth and elevation respectively. In 2ω mode, only the lower deck of C3 is considered to be misaligned and for misalignment of C1 or C2 the resulting pointing error in the semi-compressed pulse is considered to be corrected prior to frequency doubling.

Table 5 title

Estimated tolerances (/mm) for (single-pass equivalent) grating separation in 1ω mode and 2ω mode in the advanced scheme

Table 5 caption

Tolerances are based on a nominal 10% loss of peak power on target.

Table 6 title

Estimated tolerances for beam pointing into the 1ω pulse compression in 1ω mode and 2ω mode in the advanced scheme

Table 6 caption

Tolerances are based on a nominal 10% loss of peak power on target. In 2ω mode, the tolerances reflect the effect of misalignment on the operation of the grating pairs only. The direct effect of pointing error on the frequency doubling process is excluded.

Table 7 title

Estimated tolerances (/μrad) for the angle between the beam within the frequency doubling crystals and the optical axis of the material in 2ω mode in the advanced scheme

Table 7 caption

Tolerances are based on a nominal 10% loss of either energy or peak power on target.